

# Preparation and characterization of anti-tissue factor single-chain variable fragment antibody for cancer diagnosis

Ryuta Sato,<sup>1,2</sup> Toshifumi Obonai,<sup>1,2</sup> Ryo Tsumura,<sup>1,2</sup> Kouhei Tsumoto,<sup>3</sup> Yoshikatsu Koga,<sup>1</sup> Masahiro Yasunaga<sup>1</sup> and Yasuhiro Matsumura<sup>1,2</sup>

<sup>1</sup>Division of Developmental Therapeutics, Research Center for Innovative Oncology, National Cancer Center Hospital East, Chiba; <sup>2</sup>Laboratory of Cancer Biology, Department of Integrated Biosciences, Graduate School of Frontier Sciences, The University of Tokyo, Chiba; <sup>3</sup>Medical Proteomics Laboratory, Institute of Medical Science, The University of Tokyo, Tokyo, Japan

## Key words

Cancer diagnosis, molecular imaging, monoclonal antibody, single-chain variable fragment, tissue factor

## Correspondence

Yasuhiro Matsumura, Division of Developmental Therapeutics, Research Center for Innovative Oncology, National Cancer Center Hospital East, 6-5-1 Kashiwanoha, Kashiwa 277-8577, Japan.  
Tel/Fax: +81-4-7134-6857;  
E-mail: yhmatsum@east.ncc.go.jp

## Funding information

National Cancer Center Research and Development Fund (23-A-45). (26-A-12). Japan Society for the Promotion of Science (JSPS) through the Funding Program for World-Leading Innovative R&D on Science and Technology

Received August 26, 2014; Revised October 6, 2014; Accepted October 7, 2014

Cancer Sci 105 (2014) 1631–1637

doi: 10.1111/cas.12557

Venous thromboembolism (VTE) and disseminated intravascular coagulation (DIC) are serious complications in cancer patients.<sup>(1,2)</sup> Tissue factor (TF) initiates the extrinsic blood coagulation cascade by binding to coagulation factor VII and converting it to its active form (VIIa); the complex formed between TF and factor VIIa initiates the blood coagulation cascade.<sup>(3–5)</sup> Tissue factor is known to be expressed at high levels in several types of tumors, not only on tumor cell surface, but also in the stromal cells, including the tumor vascular endothelial cells.<sup>(6,7)</sup> Therefore, anti-TF antibody can target both the cancer cells and the stroma of tumors.

Recently, molecular imaging by MRI, PET and single photon emission computed tomography (SPECT) has attracted much attention in cancer research, e.g., in the study of cancer biology, drug development and cancer diagnosis. Various probes to visualize tumors have been developed and used in clinical practice to date. Antibodies are expected to serve as magic bullets in the field of molecular imaging of tumors. In addition to tumor specificity, the convenience of use and lack of toxicity are also strongly desired characteristics of molecular probes, because tools for cancer diagnosis are often used on healthy populations in the outpatient setting. IgG probes have certain undesirable properties such as long circulation

Tissue factor (TF), which serves as the initiator of the extrinsic blood coagulation cascade, has been found to be overexpressed in various solid tumors, especially brain tumors, pancreatic cancer, and gastric cancer. Overexpression of TF is considered to contribute to the high incidence of thrombotic complications and poor prognosis in patients with such cancers. Therefore, detection or targeting of TF may be a promising approach for the diagnosis and treatment of solid tumors that are known to overexpress the protein. Here, we used the recombinant DNA technology to develop an anti-TF single-chain Fv (scFv) of small size and high affinity for its target. The biochemical characteristics of the anti-TF scFv were evaluated using surface plasmon resonance (SPR) sensing and flow cytometry. The data obtained showed that the affinity of the anti-TF scFv was  $2.04 \times 10^{-8}$  (KD), and that the protein showed significant binding to the cancer cells. Then, Alexa 647-labeled anti-TF scFv and anti-TF IgG were administered to mice bearing chemically induced spontaneous tumors. The maximum tumor to background ratios of anti-TF scFv and anti-TF IgG were obtained 3 and 24 h after the injections, respectively. This study indicates anti-TF scFv may be suitable as an imaging probe for the diagnosis of solid tumors.

time in the blood and distribution to the liver. In addition, it is well known that intact IgG cannot penetrate to the center of the tumor tissue in the presence of the dense stromal barrier.<sup>(8)</sup> To overcome these drawbacks, protein engineering has been applied to reduce the probe size to obtain better tumor penetration as compared to the original IgG.<sup>(8–10)</sup> IgG can be converted to F(ab')<sub>2</sub>, Fab and a single-chain variable fragment (scFv). Both F(ab')<sub>2</sub> and Fab are produced by enzymatic digestion. On the other hand, scFv is obtained by recombinant DNA technology.<sup>(11)</sup> ScFv is a fusion protein composed of the heavy (VH) and light (VL) chains of an antibody with a flexible peptide linker that covalently joins the VH and VL domains in a single peptide. However, scFv often shows lower antigen-binding activity as compared to the original IgG.<sup>(12)</sup> In the present study, we produced anti-TF scFv and evaluated its usefulness as a molecular imaging probe for medical use.

## Materials and Methods

**Cell lines.** LTPA, a murine pancreatic cancer cell line, and BxPC3, a human pancreatic cell line, were purchased from American Type Culture Collection (ATCC, Manassas, VA, USA). To obtain LTPA cells showing high expression levels

of mouse TF (mTF) (LTPA-TF), the mTF gene was cloned into a pEF6 vector (Invitrogen, Carlsbad, CA, USA), followed by transfection of the LTPA cells with the expression vector. LTPA-TF cells stably expressing mTF were obtained by selection using the drug blastocidin. The cells were maintained in RPMI1640 (Wako, Osaka, Japan) supplemented with 10% FBS (Gibco, NY, USA) and 100 units/mL Penicillin, 100 µg/mL Streptomycin and 0.25 µg/mL Amphotericin B suspension (Wako) in an atmosphere containing 5% CO<sub>2</sub> at 37°C.

**Production of anti-mTF scFv.** Anti-mTF mAb, clone 1157, was developed by us. Total RNA was extracted from clone 1157 hybridoma cells and cDNA was synthesized from the total RNA. The cDNA of the 1157 VL and VH were then amplified by PCR (a thermal cycling program consisting of 35 cycles of 94°C for 15 s, 55°C for 15 s, and 68°C for 1 min using mix primers, according to the method described in a previous report.<sup>(13)</sup> Each amplified product was then re-amplified using the following primers to add restriction enzyme sites: 5' CATGCCATGGGGACATTGTGTTAACACAGTCTCC 3' (forward) and 5' GGCGGCGGCTGATTTCAGTTTGGTC CCCCTCC 3' (reverse) for VL, and 5'GGATATCGAGGT GATGTTGGTGGAGTCGGGAGGAG 3' (forward) and 5' TCCCGGCGGCTGAGGAGACTGTGACCATGACTCCT 3' (reverse) for VH. A 6-His tag and Cys residues were fused, and the commonly used linker (Gly4-Ser)<sub>3</sub> was set between the VL and VH. Finally, this expression vector was designated as the pRA2 vector (Fig. 1). The anti-mTF scFv expression vector was transfected into *Escherichia coli* BL21 (Takara Bio, Tokyo, Japan), followed by incubation of the bacterial cells at 37°C for 18 h on LB-agar (Takara Bio) containing 200 µg/mL ampicillin (Wako). And then the selected cells were allowed to grow in 2 × YT medium containing 200 µg/mL ampicillin until the turbidity level reached 0.6 at O.D. 600. Then, isopropyl β-D-1-thiogalactopyranoside was added into the medium to become 500 µM. The cells were then cultured at 37°C for further 6 h, harvested by centrifugation (8000 g, 30 min, 4°C), and suspended in a buffer composed of 500 mM NaCl and 20 mM Tris-HCl (pH 8.0 at 4°C). The pellet was sonicated (model UD-201, TOMY, Tokyo, Japan) and then centrifuged (10 000 g, 30 min, 4°C) to separate the supernatant (soluble form) from the pellet (insoluble form). The supernatant was then collected and loaded onto Ni-NTA agarose (Invitrogen). The agarose was washed with a sonication buffer containing 5 mM imidazole. The anti-mTF scFv was eluted with 10, 20, 50, 100, 200, 300 and 500 mM imidazole. The eluate was filtered via Millex-GP (0.22 µm, PES, Merck-Millipore, Darmstadt, Germany). The solution was loaded on to a Superdex75 column (GE Healthcare, Uppsala, Sweden) equilibrated with phosphate buffered saline (PBS). Each fraction was analyzed by SDS-PAGE. The purified anti-mTF scFv and IgG were stored at 4°C until use. The anti-mTF scFv was transferred to a PVDF membrane (Bio-Rad Laboratories, Hercules, CA, USA), which was blocked with 0.3% Difco skim milk (Becton Dickinson, Franklin Lakes, NJ, USA) in PBS. The membranes were then incubated in the presence of 2 µg/mL anti-His-tag mAb conjugated with peroxidase (Wako) and 0.3% skim milk

in PBS for 10 min at room temperature (RT). After washing with PBS containing 0.1% Tween 20 (PBS-T, Sigma, St. Louis, MO, USA), the protein on the membranes was visualized using ECL prime (GE Healthcare) as substrate. Optical imaging was carried out with the Chemidoc XRS+ system (Bio-Rad Laboratories).

**Fluorescence labeling of scFv and IgG.** Each of the anti-mTF scFv and IgG was conjugated with Alexa 647 using the Micro-scale Protein Labeling kit (Invitrogen) and Alexa Fluor 647 protein labeling kit (Invitrogen), according to the manufacturer's instructions. The concentration of protein and fluorescence were determined by measuring the absorbance at 280 and 650 nm, respectively.

**Affinity of the anti-mTF scFv and IgG to the mTF antigen.** The interactions between the anti-mTF mAbs and mTF protein were analyzed by surface plasmon resonance (SPR) sensing using Biacore T200 (GE Healthcare), according to the manufacturer's instructions. As a running buffer, HBS-EP+ buffer (GE Healthcare) was degassed before use. The purified mTF protein solution in 10 mM Na-Acetate, pH 5.0 (GE Healthcare) was immobilized on to the sensor surface of a Biacore sensor chip CM5 (GE Healthcare) to immobilized ligand densities (RU) of about 1600 for anti mTF scFv and about 20 for anti mTF IgG, using an amine coupling kit. Then, anti-mTF mAb at concentrations of 10–160 nM was allowed to flow through the sensor chip. The BIA evaluation software (GE Healthcare) assuming the Langmuir 1:1 binding model was used to analyze the data. The affinity (KD) was calculated using the following formula; KD = dissociation rate constant (kd)/association rate constant (ka).

**Flow cytometric analysis.** The antigen-binding activities of the anti-mTF mAbs (scFv and IgG) using LTPA and LTPA-TF and BxPC3 were analyzed by Guava (Merck-Millipore). In 5-mL tubes, 2.0 × 10<sup>5</sup> cells were incubated with 35.7 p mol of each of the mAbs labeled with alexa 647 (50.3 p mol dye for scFv and 112.5 dye for IgG) for 30 min at 4°C. After washing with PBS containing 0.5% BSA and 2 mM EDTA (B.E. PBS), the cells were stained with PI solution (Invitrogen). The flow cytometry data were analyzed by FLOWJO, a flow cytometry software (Tree Star, Ashland, OR, USA). The isotype IgG was used as a control.

**Inhibition assay.** 17.9 p mol the scFv of the labeled with alexa 647 were incubated with 0, 19.2, 192 p mol recombinant soluble mTF antigen for 30 min at 4°C, respectively. 2.1 p mol the IgG labeled with alexa 647 were incubated with 0, 19.2 or 192 p mol recombinant soluble mTF antigen for 30 min at 4°C, respectively. In 5-mL tubes, 2.0 × 10<sup>5</sup> LTPA-TF cells were incubated with the reaction solution for 30 min at 4°C. After washing with B.E.PBS, the cells were stained with PI solution (Invitrogen). Flow-cytometric analysis was described above all.

**Chemically induced mouse cutaneous cancer.** A mouse model of cutaneous cancer induced by a chemical carcinogen was produced by a previously described method.<sup>(14)</sup> Briefly, a single application of 7,12 dimethylbenz[α]anthracene (DMBA; 250 µg/mL in acetone; Sigma) was made to the shaved dorsal skin of 6-week-old female FVB/N mice. After 1 week, phorbol 12-myristate 13-acetate (PMA; 25 µg/mL in acetone; Sigma) was applied to the skin weekly. The experiments of the present study were conducted when the tumor volume reached approximately 200 mm<sup>3</sup>. The tumor volume (TV) was calculated from the length (L) and width (W) of the subcutaneous tumor using the following formula: TV = (L × W<sup>2</sup>)/2.

**Immunohistochemistry.** When the tumor volume in the animals reached over 200 mm<sup>3</sup>, the tumors were excised under

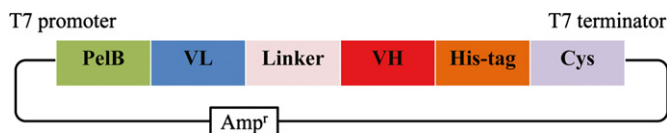


Fig. 1. Plasmid construction of the single-chain variable region (scFv).

deep anesthesia. Then, they were embedded in Tissue-Tek OCT (Sakura Finetek, Tokyo, Japan) and frozen on dry ice. The tumor specimens were sectioned with a cryostat3 DM (Sakura Finetek) on Microslides (Muto Pure Chemicals, Tokyo, Japan) into sections of 10- $\mu$ m thickness. After washing with PBS, the sections were fixed with 4% paraformaldehyde for 15 min at RT. They were then washed with PBS and their endogenous peroxidase activities were blocked with 0.3% hydrogen peroxide solution in methanol for 20 min. The blocking was conducted with 3% skim milk in PBS for 1 h. The sections were incubated with anti-mTF antibody (2  $\mu$ g/mL) as the first antibody for 1 h at RT. Then, after washing with PBS, they were incubated with anti-rat IgG-HRP (Histostar, MBL, Nagoya, Japan) as a second antibody for 1 h at RT. Then, after washing again with PBS, the sections were incubated with DAB (Dako, Glostrup, Denmark) for 1 min. They were counterstained with H&E. Optical imaging was carried out with the confocal microscope BZ-9000 (Keyence, Osaka, Japan).

**In vivo tumor imaging.** When the tumor volume reached over 200 mm<sup>3</sup>, 100  $\mu$ L of 6.67  $\mu$ M fluorescence-labeled anti-mTF scFv or IgG was injected via the mouse tail vein. *In vivo* fluorescence imaging was performed with an IVIS *in vivo* imaging system (Caliper Life Sciences, Hopkinton, MA, USA) at 0.5, 1, 3, 6, 12, 24 and 72 h after the injection. (Ex/Em = 604/640). The measurements of the fluorescence intensity were performed as described previously.<sup>(15)</sup> Image analysis was carried out using the IVIS software by drawing a region of interest around each tumor and the average intensity was obtained. The tumor staining intensity was calculated using following formula; tumor intensity = (post-injection tumor intensity) – (pre-injection tumor intensity). The average intensity of the background was measured in the back skin on the side back of the back skin contralateral to the tumor. The tumor-background ratio (TBR) was calculated using the following formula; TBR = (post injection tumor intensity)/(post injection back ground intensity). The control scFv used was HyHEL10 scFvLH, directed against hen egg-white lysozyme (HEL).<sup>(16)</sup>

All animal procedures were carried out in compliance with the Guideline for the Cancer and Use of Experimental Animals established by the Committee for Animal Experimentation from the National Cancer Center, Japan. These guidelines meet the ethical standards required by law and also comply with the guidelines for the use of experimental animals in Japan.

## Results

**Development of anti-mTF scFv.** We determined the sequences of the VH and VL regions of our anti-mTF monoclonal antibody. The specificity was validated using IGBLAST, according to the method described in a previous report.<sup>(17,18)</sup> The construction of anti-mTF scFv is shown in Figure 1. Western blot analysis showed that the anti-mTF scFv was expressed in a soluble form in the supernatant of the cell lysate and in an insoluble form in the inclusion bodies (Fig. 2a). The anti-mTF scFv with a 6-His tag was purified using affinity chromatography and size-exclusion chromatography. The results of size-exclusion chromatography indicated that there were monomers and dimers of the anti-mTF scFv in the supernatant (Fig. 2b). Finally, the monomer scFv, which represented the single-chain protein as judged by visualization of a single band of 28 kDa on SDS-PAGE, was purified and used for this study (Fig. 2c).

**The binding assay.** The binding activity of anti-mTF scFv was evaluated by SPR sensing. An increase in the SPR signal (expressed in response units, RU) was observed from 10 to 160 nM (Fig. 3a), for both anti-mTF scFv and IgG. The dissociation constant (kd) of anti-mTF scFv was higher than that of IgG, while its association constant (ka) was lower than that of IgG. Consequently, anti-mTF scFv had binding affinity with a dissociation constant (KD) value of about  $2.04 \times 10^{-8}$ , comparable to that of the original anti-mTF IgG (clone 1157; dissociation constant,  $4.82 \times 10^{-10}$ ) (Table 1). We then confirmed the specificity of anti-mTF scFv and IgG on the LTPA-TF cells. Soluble mTF antigen inhibited the scFv and IgG binding activity, significantly (Fig. 3b). The binding of both mAbs to cells appeared to depend on the mTF expression on the cells (Fig. 3c). Furthermore, fluorescence intensity on the LTPA-TF cells of anti-mTF scFv was below one-tenth of that of the IgG. These results indicated the reduced binding activity of the scFv as compared with original IgG.

**In vivo imaging.** Initially we tried to use mouse pancreatic tumor cell LTPA and TF overexpressing LTPA to examine the distribution of the anti-TF scFv and IgG. These murine cells, however, could not grow in the body of any types of mice including nude, Scid, NOD-Scid, and NOG mice. These anti-mTF mAbs did not cross-react with the TF on human pancreatic cancer cells, BxPC3 (Fig. S1). Instead, mice bearing chemically induced spontaneous cutaneous tumors were selected for evaluation of the distribution of the anti-mTF IgG and scFv, because the spontaneous tumors contained abundant stroma, similar to the case of human cancer. These tumors

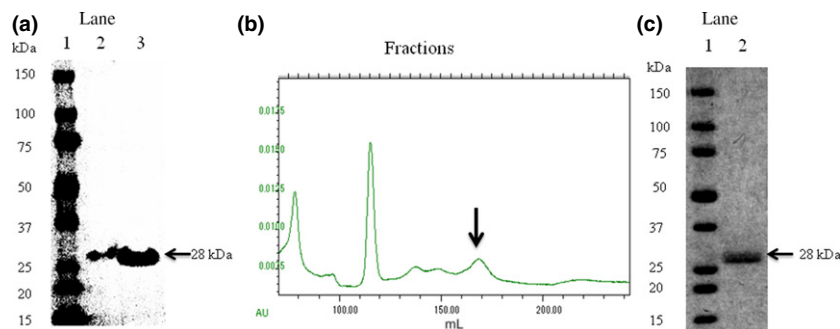


**Fig. 2.** Purification of anti-mTF scFv. Anti-mTF scFv was produced in an *Escherichia coli* system and purified by gel-filtration chromatography. (a) Western blotting of anti-mTF scFv with anti-His-tag antibody. lane1: size marker; lane2: soluble form of anti-mTF scFv; lane3: solubilized anti-mTF scFv in an inclusion body. Arrow indicates 28 kDa band. (b) Size-exclusion chromatography following nickel affinity chromatography of the soluble anti-mTF scFv. There were monomers (arrow) and dimers of anti-mTF scFv. (c) SDS-PAGE. CBB staining of purified anti-mTF scFv. Lane 1: size marker; lane 2: anti-mTF scFv. Arrow indicates 28 kDa.

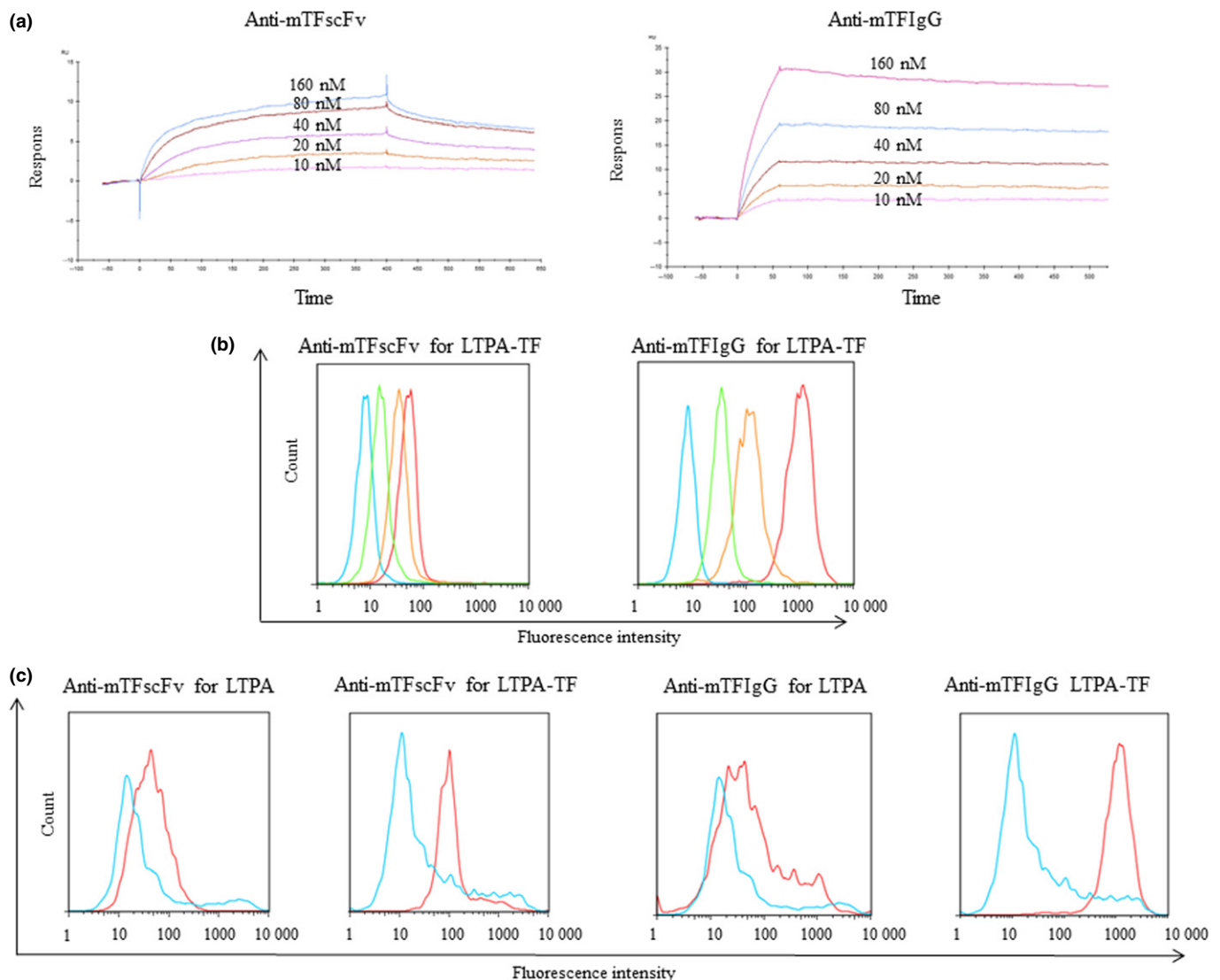


**Fig. 3.** Binding activity of anti-mTF scFv evaluated by SPR sensing and flow cytometry. (a) Binding plots of anti-mTF scFv and IgG by SPR imaging. Different concentrations of the monomeric fractions of anti-mTF scFv or IgG were injected on the Biacore chip with mTF antigen immobilized on it. An increase in SPR signal was observed from 10 to 160 nM for both antibodies. The association of anti-TF scFv with the mTF antigen was slower than that of IgG. The dissociation of anti-mTF scFv from the antigen was faster than that of the IgG. (b) Flow cytometry using LTPA-TF and inhibition assay of the anti-mTF mAbs. Anti-mTF scFv showed specific mTF binding. Soluble mTF antigen inhibited the binding activity of dye labeled anti-mTF scFv (17.9 pmol, left) and anti-mTF IgG (2.1 pmol, right). 0 pmol (red), 19.2 pmol (yellow) or 192 pmol (green) mTF was added for scFv or IgG. Blue indicates negative control (left and right). (c) Flow cytometry using LTPA cells and LTPA-TF cells. Anti-mTF scFv showed specific mTF binding. Its binding activity, however, was lower than that of the original IgG. Red, anti-mTF antibody (anti-mTF scFv or IgG). Blue, control antibody.

**Table 1.** Comparison of  $k_a$ ,  $k_d$  and  $K_D$  between the anti-mTF scFv and the anti-mTF IgG

	$k_a$	$k_d$	$K_D$
Anti-TF scFv	$7.44 \times 10^4$	$1.52 \times 10^{-3}$	$2.04 \times 10^{-8}$
Anti-TF IgG	$1.67 \times 10^5$	$8.07 \times 10^{-5}$	$4.82 \times 10^{-10}$

showed ulcerative and hemorrhagic change in gross appearance (Fig. 4a). HE staining showed that these tumors had abundant tumor stroma (Fig. 4b, left). Moreover, the immunohistochemistry with anti-mTF mAb indicated remarkable mTF expression in the cancer region, especially at the invasion site (Fig. 4b,c, right). Systemic *in vivo* imaging revealed that while control scFv did not accumulate in the tumors, anti-mTF scFv showed selective accumulation in the tumor from 1 h after the

injection, and was eliminated from the body by 12 h after the injection (Fig. 4d,e). On the other hand, anti-mTF IgG showed selective accumulation in the tumor for over 72 h (Fig. 4d,e). The TBR of anti-mTF scFv was maximal at 3 h after the injection. On the other hand, that of anti-TF IgG was maximal at 24 h after the injection (Fig. 4f).

### Discussion

In this study, we succeeded in developing a high-affinity scFv specific for mTF. Cysteine was added to the C terminal of anti-mTF scFv as the reactive residue for the drug conjugation.<sup>(19)</sup> While various kinds of scFvs have been produced until date, scFv appears to have a lower affinity for the target antigen as compared to the original IgG, and to exist in inclusion bodies in *Escherichia coli*. In the latter case, denaturation

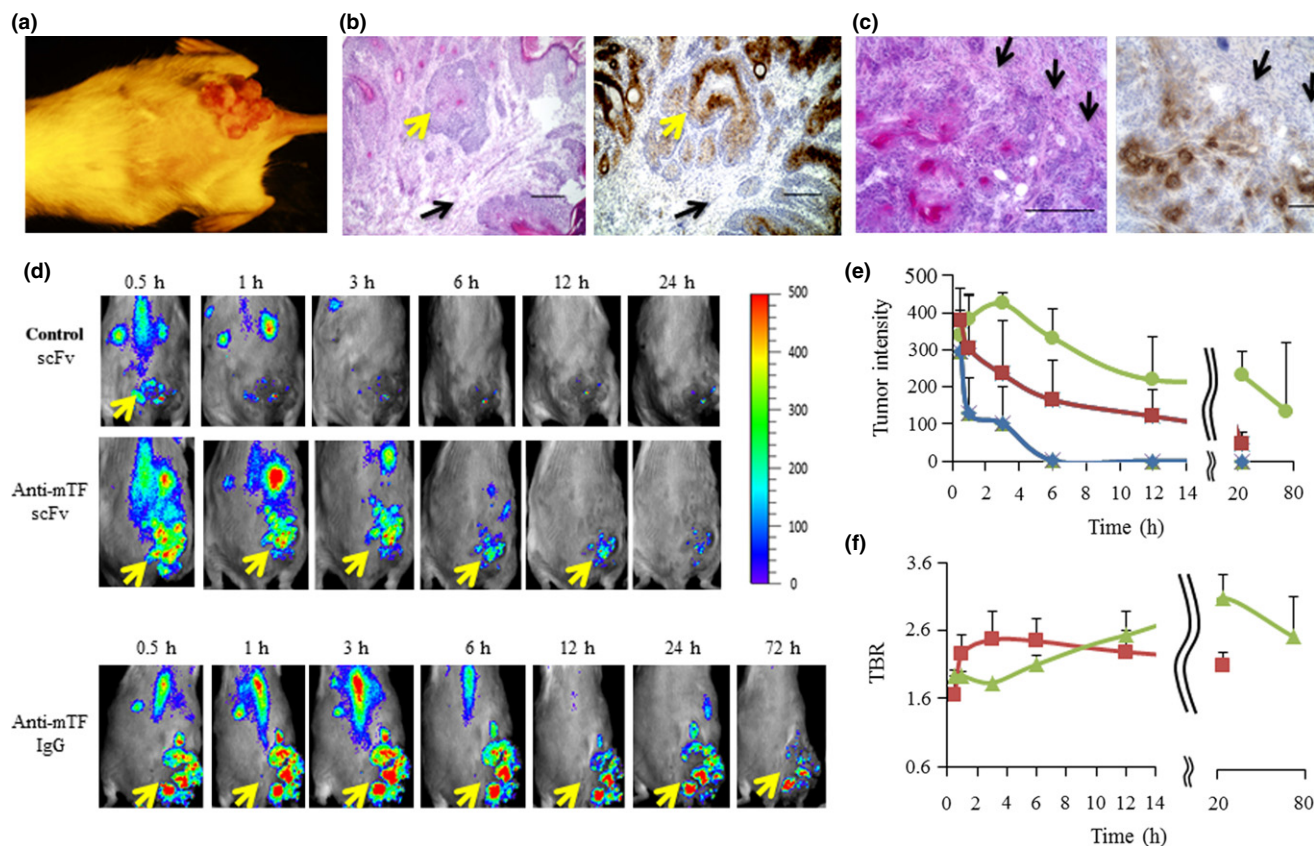


**Fig. 4.** *In vivo* imaging of anti-mTF scFv and IgG. (a) Massive spontaneous cutaneous tumors were developed on mice back. These tumors showed partially ulcerative and hemorrhagic change. (b) HE staining for the tumor cell clusters and tumor stroma (left). These tumor had abundant tumor stroma. The immunohistochemistry with anti-mTF mAb showed remarkable mTF expression in the tumor region (right). Yellow arrow denotes tumor cells clusters. Black arrow denotes cancer stroma. Scale bar: 200  $\mu$ m. (c) HE staining for the invasion site of the squamous cancer cell clusters. Arrows denote tumor cells invasion site into stroma (left). The immunohistochemistry with anti-mTF mAb showed remarkable mTF expression in the cancer invasion region (right). Arrows indicated tumor cells invasion site into stroma. Scale bar: 200  $\mu$ m. (d) *In vivo* imaging for accumulation of control scFv, anti-mTF scFv and anti-mTF IgG. The tumors are indicated by yellow arrows. (e) Fluorescence intensities in the tumor for control scFv (blue), anti-mTF scFv (red) and anti-mTF IgG (green) were measured ( $n = 3$  tumor areas per time-point). Selective accumulation of anti-mTF scFv was seen at 1 h after the injection, and eliminated from the body by 12 h after the injection. On the other hand, selective accumulation of anti-mTF IgG in the tumor was observed for over 72 h. (f) Comparison of the tumor to background ratio (TBR) between anti-mTF scFv and IgG ( $n = 3$  tumor areas per time-point). The TBR of anti-mTF scFv was maximal at 3 h after the injection; on the other hand, that of anti-TF IgG was at 24 h after the injection.

with guanidine hydrochloride followed by refolding is required.<sup>(20,21)</sup> Because our anti-mTF scFv existed in the soluble form in *E. coli*, anti-mTF scFv could be easily obtained at high purity, as confirmed by the visualization of a single band in the SDS-PAGE analysis.

We evaluated the antigen-binding activity of anti-mTF scFv by SPR sensing. In comparison to the original anti-mTF IgG ( $KD = 4.82 \times 10^{-10}$ ), anti-mTF scFv showed a higher  $k_d$  and lower  $k_a$ , with a  $KD$  value of  $2.04 \times 10^{-8}$ . The increased  $k_d$  value may mostly be attributable to the single antigen-binding site of anti-mTF scFv as compared to the bivalent binding activity of the original IgG. Until now, scFv with  $KD$  values ranging from  $1 \times 10^{-9}$  to  $1 \times 10^{-7}$  has been used for cancer imaging,<sup>(11,12,22)</sup> and the  $KD$  value of our scFv was  $2.04 \times 10^{-8}$ , which appears to be acceptable for accurate cancer imaging.

High TF expression is reported in many human cancers, including glioblastoma, pancreatic cancer, gastric cancer, etc. However, there is little knowledge in relation to mouse tumor cells showing high expression levels of TF. Therefore, we prepared LTPA cells (a murine pancreatic cancer cell line) over-expressing mTF (LTPA-TF) by stable transfection of an mTF

gene-inserted plasmid. The flow-cytometric analysis confirmed the specific binding of the scFv to the mTF antigen (Fig. 3a, b). Moreover, the scFv binding to cells appeared to depend on mTF expression on the cell surface (Fig. 3c). We also selected the mouse model of chemically induced cutaneous cancer as the appropriate experimental model for evaluating the feasibility of cancer diagnosis using anti-mTF scFv, because this spontaneous tumor shows high expression levels of mTF and an abundant tumor stroma, similar to the case in human solid cancers, in general. We also found high expression levels of mTF especially in the invasion site of cancer clusters, which are well-differentiated squamous cell carcinoma (SCC). In addition, this spontaneous tumor is very slow in tumor growth and lastly metastasized to other organs to kill host mice in almost a year that are also more similar to general clinical human cancer as compared to the xenografts.<sup>(23)</sup>

The *in vivo* imaging study showed that the control scFv disappeared within 3 h after the injection and showed no clear tumor accumulation. On the other hand, anti-mTF scFv accumulated and was retained in the tumors from 1 to 12 h after the injection. Moreover, it showed a high tumor to normal tissue background ratio and early body clearance as compared to the original IgG.

The peak of the TBR signal with anti-mTF scFv was recognized at 3 h after the injection. On the other hand, that of IgG was observed at 24 h after the injection. The molecular size of IgG is 150 kDa; therefore, IgG cannot pass through the glomeruli of the kidney and has a long half-life in the body.<sup>(24)</sup> Moreover, IgG can accumulate in the tumor for a long time, on the basis of the EPR effect.<sup>(25)</sup> In contrast, small-sized (28 kDa) scFv, which lacks the Fc, cannot benefit from the EPR effect, resulting in a more rapid body clearance and faster TBR peak. These features indicate that IgG and scFv have suitable characteristics as delivery tools for cancer therapy and diagnosis, respectively.

Although anti-Her2 scFvs for molecular imaging have already been reported, the number of Her2-positive cancer patients is limited.<sup>(26,27)</sup> Therefore, it could be applied for the prediction of the therapeutic response to anti-HER2 antibody rather than for the general diagnosis of cancer. In contrast, TF is expressed at a high frequency in various types of cancers and their stroma. Therefore, anti-TF scFv may be applied for the diagnosis of a wide range of cancers. Moreover, the TF expression level is known to be correlated with a poor prognosis.<sup>(28)</sup> Detection of TF expression may also be considered to be useful to predict serious complications such as VTE. Meanwhile, for diagnostic use in clinical practice, the safety and examination time should also be considered, because the diagnostic test is also applied to healthy people or outpatients. IgG contains the constant Fc region, which triggers immune response to a given antigen and may cause serious allergic reactions. Therefore, it is clear that scFv lacking Fc is safer than IgG in this regard. An anti-mTF IgG has been reported for use in PET imaging;<sup>(29)</sup> it takes a few days to complete the imaging, which would be inconvenient for outpatients. Small-sized scFvs, showing faster clearance and providing a faster peak signal to noise ratio, allow the test to be completed in only half a day. In addition, they also reduce the exposure

levels to radionuclides. MRI is often used for the diagnosis of tumors, such as brain tumor or pancreatic cancer, which show high TF expression levels. To define tumor boundaries or identify vascular invasion, MRI with gadolinium contrast is applied. However, it is difficult to determine the tumor invasion site precisely, evaluate the tumor cell viability, or detect the tumor at an early stage by this modality. Molecular MRI using a targeted contrast with antibody is expected to increase both the resolution and the sensitivity of imaging, as next-generation clinical imaging. The results of this study showed that anti-mTF scFv can bind to mTF-positive cancer cells. Moreover, rapid clearance is beneficial to minimize the gadolinium toxicity. Therefore, anti-TF scFv is a highly promising candidate as a targeting probe for MRI.

In conclusion, our anti-mTF scFv exhibited rapid renal clearance and faster selective intratumor accumulation after the injection. Thus, anti-TF scFv may be a suitable imaging tool for the diagnosis of refractory solid tumors.

### Acknowledgements

This work was supported by the National Cancer Center Research and Development Fund (23-A-45 to Y. Matsumura and 26-A-12 to M. Yasunaga) and a Grant-in-Aid from the Japan Society for the Promotion of Science (JSPS) through the Funding Program for World-Leading Innovative R&D on Science and Technology (FIRST Program), initiated by the Council for Science and Technology Policy (CSTP) (to Y. Matsumura), Center of Innovation (COI) Program from Japan Science and Technology Agency (JST) (M.Y. asunaga) and we thank to Mrs. M. Kanzaki for supporting animal experiments and to Mrs. K. Shiina for secretarial support.

### Disclosure Statement

The authors have no conflict of interest.

### References

- Blom JW, Doggen CJ, Osanto S, Rosendaal FR. Malignancies, prothrombotic mutations, and the risk of venous thrombosis. *JAMA* 2005; **293**: 715–22.
- Thaler J, Koder S, Kornek G, Pabinger I, Ay C. Microparticle-associated tissue factor activity in patients with metastatic pancreatic cancer and its effect on fibrin clot formation. *Transl Res* 2013; **163**: 145–50.
- Hoffman M, Colina CM, McDonald AG, Arepally GM, Pedersen L, Monroe DM. Tissue factor around dermal vessels has bound factor VII in the absence of injury. *J Thromb Haemost* 2007; **5**: 1403–8.
- Jesty J, Beltrami E. Positive feedbacks of coagulation: their role in threshold regulation. *Arterioscler Thromb Vasc Biol* 2005; **25**: 2463–9.
- Drake TA, Morrissey JH, Edgington TS. Selective cellular expression of tissue factor in human tissues. Implications for disorders of hemostasis and thrombosis. *Am J Pathol* 1989; **134**: 1087–97.
- Rong Y, Post DE, Pieper RO, Durden DL, Van Meir EG, Brat DJ. PTEN and hypoxia regulate tissue factor expression and plasma coagulation by glioblastoma. *Cancer Res* 2005; **65**: 1406–13.
- Abe K, Shoji M, Chen J *et al.* Regulation of vascular endothelial growth factor production and angiogenesis by the cytoplasmic tail of tissue factor. *Proc Natl Acad Sci USA* 1999; **96**: 8663–8.
- Tang Y, Wang J, Scollard DA *et al.* Imaging of HER2/neu-positive BT-474 human breast cancer xenografts in athymic mice using 111In-trastuzumab (Herceptin) Fab fragments. *Nucl Med Biol* 2005; **32**: 51–8.
- Schaefer JV, Pluckthun A. Transfer of engineered biophysical properties between different antibody formats and expression systems. *Protein Eng Des Sel* 2012; **25**: 485–506.
- Labrijn AF, Meesters JI, de Goeij BE *et al.* Efficient generation of stable bispecific IgG1 by controlled Fab-arm exchange. *Proc Natl Acad Sci USA* 2013; **110**: 5145–50.
- Adams GP, Schier R. Generating improved single-chain Fv molecules for tumor targeting. *J Immunol Methods* 1999; **231**: 249–60.
- Cyranka-Czaja A, Wulhfard S, Neri D, Otlewski J. Selection and characterization of human antibody fragments specific for psoriasis – a cancer associated protein. *Biochem Biophys Res Comm* 2012; **419**: 250–5.
- Andris-Widhopf J, Steinberger P, Fuller R, Rader C, Barbas CF 3rd. *Phage Display A Laboratory Manual*. New York, NY: CSH Press, 2011; 53–64.
- Yasunaga M, Manabe S, Matsumura Y. New concept of cytotoxic immun-conjugate therapy targeting cancer-induced fibrin clots. *Cancer Sci* 2011; **102**: 1396–402.
- Thurber GM, Weissleder R. Quantitating antibody uptake *in vivo*: conditional dependence on antigen expression levels. *Mol Imaging Biol* 2011; **13**: 623–32.
- Tsumoto K, Nakaoki Y, Ueda Y *et al.* Effect of the order of antibody variable regions on the expression of the single-chain HyHEL10 Fv fragment in *E. coli* and the thermodynamic analysis of its antigen-binding properties. *Biochem Biophys Res Comm* 1994; **201**: 546–51.
- Proba K, Worn A, Honegger A, Pluckthun A. Antibody scFv fragments without disulfide bonds made by molecular evolution. *J Mol Biol* 1998; **275**: 245–53.
- Ye J, Ma N, Madden TL, Ostell JM. IgBLAST: an immunoglobulin variable domain sequence analysis tool. *Nucleic Acids Res* 2013; **41**: W34–40.
- Wakankar AA, Feeney MB, Rivera J *et al.* Physicochemical stability of the antibody-drug conjugate Trastuzumab-DM1: changes due to modification and conjugation processes. *Bioconjug Chem* 2010; **21**: 1588–95.
- Sushma K, Bilgimol CJ, Vijayalakshmi MA, Satheshkumar PK. Recovery of active anti-TNF- $\alpha$  ScFv through matrix-assisted refolding of bacterial inclusion bodies using CIM monolithic support. *J Chromatogr B Analyt Technol Biomed Life Sci* 2012; **891–892**: 90–3.
- Fukunaga A, Tsumoto K. Improving the affinity of an antibody for its antigen via long-range electrostatic interactions. *Protein Eng Des Sel* 2013; **26**: 773–80.
- Zhou Y, Drummond DC, Zou H *et al.* Impact of single-chain Fv antibody fragment affinity on nanoparticle targeting of epidermal growth factor receptor-expressing tumor cells. *J Mol Biol* 2007; **371**: 934–47.
- Hisada Y, Yasunaga M, Hanaoka S *et al.* Discovery of an uncovered region in fibrin clots and its clinical significance. *Sci Rep* 2013; **3**: 2604.

- 24 Chen B, Jerger K, Frechet JM, Szoka FC Jr. The influence of polymer topology on pharmacokinetics: differences between cyclic and linear PEGylated poly(acrylic acid) comb polymers. *J Control Release* 2009; **140**: 203–9.
- 25 Matsumura Y, Maeda H. A new concept for macromolecular therapeutics in cancer chemotherapy: mechanism of tumorotropic accumulation of proteins and the antitumor agent smancs. *Cancer Res* 1986; **46**: 6387–92.
- 26 Olafsen T, Tan GJ, Cheung CW *et al.* Characterization of engineered anti-p185HER-2 (scFv-CH3)<sub>2</sub> antibody fragments (minibodies) for tumor targeting. *Protein Eng Des Sel* 2004; **17**: 315–23.
- 27 Zdobnova TA, Stremovskiy OA, Lebedenko EN, Deyev SM. Self-assembling complexes of quantum dots and scFv antibodies for cancer cell targeting and imaging. *PLoS ONE* 2012; **7**: e48248.
- 28 Lima LG, Monteiro RQ. Activation of blood coagulation in cancer: implications for tumor progression. *Biosci Rep* 2013; **33**: arte00064.
- 29 Hong H, Zhang Y, Nayak TR *et al.* Immuno-PET of tissue factor in pancreatic cancer. *J Nucl Med* 2012; **53**: 1748–54.

## Supporting Information

Additional supporting information may be found in the online version of this article:

**Fig. S1.** Flow cytometry using BxPC3 cells.